Plant-derived benzoxazinoids act as antibiotics and shape bacterial communities

Authors

Niklas Schandry[1,2,*], Katharina Jandrasits[1], Ruben Garrido-Oter[3], Claude Becker[1,2,*]

[1] Gregor Mendel Institute of Molecular Plant Biology, Austrian Academy of Sciences, Vienna BioCenter (VBC), 1030 Vienna, Austria

[2] Genetics, Faculty of Biology, Ludwig Maximilians University Munich, 82152 Martinsried, Germany

[3] Department of Plant Microbe Interactions, Max Planck Institute for Plant Breeding Research, 50829 Cologne, Germany

* Correspondence should be addressed to claude.becker@bio.lmu.de and niklas.schandry@bio.lmu.de

Abstract

Plants synthesize and release specialized metabolites into their environment that can serve as chemical cues for other organisms. Metabolites that are released from the roots are important factors in determining which microorganisms will colonize the root and become part of the plant rhizosphere microbiota. Root exudates are often further converted by soil microorganisms, which can result in the formation of toxic compounds. How individual members of the plant rhizosphere respond to individual compounds and how the differential response of individual microorganisms contributes to the response of a microbial community remains unclear. Here, we investigated the impact of derivatives of one class of plant root exudates, benzoxazinoids, which are released by important crops such as wheat and maize, on a collection of 180 root-associated bacteria. We show that phenoxazine, derived from benzoxazinoids, inhibits the growth of root-associated bacteria *in vitro* in an isolate-specific manner, with sensitive and resistant isolates in most of the studied clades. Synthetic bacterial communities that were assembled from only resistant isolates were more resilient to chemical perturbations than communities composed of only sensitive members. Isolates that were shared between different communities showed stable interactions, independent of the overall community composition. On the other hand, we could attribute differential community development to differences in interactions formed by closely related representatives of the same bacterial genus. Our findings highlight the fact that profiling isolate collections can aid the rational design of synthetic communities. Moreover, our data show that simplified *in vitro* community systems are able to recapitulate observations on the influence of metabolite exudation on the structure of root-associated communities, thus providing an avenue for reductionist explorations of the rhizosphere biology in defined, host-free settings.

Introduction

In the rhizosphere, the space directly surrounding the roots, plants recruit and maintain a diverse community of microorganisms that differs from the surrounding bulk soil (Bulgarelli et al., 2013, 2012; Fitzpatrick et al., 2020; Stringlis et al., 2018). These rhizospheric microbiota, in particular bacteria and fungi, contribute to plant nutrition, growth, and defense (Fitzpatrick et al., 2020).

While it is clear that there are biochemical interactions at play in the establishment and the qualitative and quantitative modulation of the microbiota, the chemical ecology of the rhizosphere is not well understood, in part owing to the biological, chemical, and physical complexity of the soil environment. Recent studies have shown, however, that some plant specialized metabolites contribute to plant species-specific community profiles in the rhizosphere. For example, salicylic acid, camalexin, coumarins, and glucosinolates play an important role in shaping the *Arabidopsis thaliana* rhizosphere (Harbort et al., 2020; Jacoby et al., 2020; Koprivova et al., 2019; Lebeis et al., 2015; Stringlis et al., 2018; Voges et al., 2019). Members of the Poaceae family (grasses), including wheat and maize, produce a particular class of specialized metabolites, the benzoxazinoids (BX) (Frey et al., 1997; Handrick et al., 2016). Chemically, BX and some of their breakdown products chelate trivalent ions and have been suggested to act as phytosiderophores in iron uptake or as protective ion scavengers (L. Hu et al., 2018). BX and their derivatives affect different branches of the tree of life: they act as herbivore repellents when stored in plant leaves, can be hijacked by nematodes to deter predators, or interfere with the growth of nearby plants (Robert et al., 2011; Schulz et al., 2013; Venturelli et al., 2016, 2015). Beyond acting on these larger-sized eukaryotes, BX exert a major influence on root-associated fungal and bacterial microbiota. For example, BX exudation by maize plants into the surrounding soil leads to conditioning of the microbiome, which in turn results in soil-memory effects that affect plants of the following sowing (Hu et al., 2018). Another

63 study showed that BX exudation specifically recruits beneficial pseudomonads to the
64 rhizosphere whereas *Comamonadaceae* are often depleted by BX exudation (Cadot et al.,
65 2020; Cotton et al., 2019; Kudjordjie et al., 2019; Neal et al., 2012; Schandry and Becker, 2020).
66 Conversely, the presence and composition of the microbiota can alter BX chemistry. Post-
67 release breakdown and metabolism of benzoxazinoid compounds by soil microbiota leads to the
68 sequential formation of 1,4-benzoxazin-3-one (BOA) and 2-amino-3-phenoxazinone (APO),
69 among other compounds, in non-sterile soils (Kumar et al., 1993; Macías et al., 2005, 2004).
70 APO in return exhibits antibiotic activity similar to other phenoxazines and limits plant root
71 growth at concentrations corresponding to those detected in soil (Anzai et al., 1960; Cheng et
72 al., 2016; Imai et al., 1990; Venturelli et al., 2016, 2015).
73 To date, the selectivity and antimicrobial activity of BX and their non-benzoxazinoid derivatives
74 such as APO on soil-dwelling and root-associated bacteria has not been systematically
75 addressed, and it remains elusive how bacterial communities respond to these compounds.
76 Given the long-term microbiome-conditioning capacity of BX exudation described above (Hu et
77 al., 2018), it is tempting to speculate that some of the plant-growth-inhibitory effects of BX
78 compounds could be mediated by selective effects on the plant-associated microbiota (Belz and
79 Hurle, 2005). However, quantitative analyses of the degree to which microbial isolates differ in
80 their response to root exudates are extremely difficult to perform in soil, because (*i*) plant-
81 associated microbiota are highly diverse, and (*ii*) plant exudates are typically complex mixtures,
82 making it difficult to attribute effects to a particular chemical. In contrast, such studies can be
83 easily carried out *in vitro* using clonal bacterial populations (isolates) and pure compounds at
84 defined concentrations.
85 Collections of culturable bacterial isolates from diverse habitats are an important resource to
86 investigate how diverse microorganisms respond to biotic and abiotic environmental cues or to
87 chemical exposure (e.g. antibiotics, toxins, or pollutants). For example, studies on the effect of
88 therapeutic drugs on an isolate collection derived from the human gut revealed isolate-specific

89 effects of non-antibiotic therapeutics on bacterial growth (Maier et al., 2018). Such collections
90 can moreover form the basis for rationally designed synthetic microbial communities (SynComs)
91 (Herrera Paredes et al., 2018; Vorholt et al., 2017). SynComs have been proposed and used as
92 reduced complexity systems to study how various microbiomes assemble and develop over
93 time (De Roy et al., 2014; Finkel et al., 2020; Liu et al., 2019; Voges et al., 2019; Vrancken et
94 al., 2019). In these studies, the function of individual members has emerged as a key predictor
95 of community function, whereas taxonomic composition appears to be less crucial. SynComs
96 have gained traction as simplified models for naturally occurring communities and are an
97 emerging tool for the targeted modulation of plant health, through holobiont (the organism
98 formed by host and microbiome) design (Trivedi et al., 2020). Bacterial SynComs in particular
99 have been adopted in plant sciences to study various aspects of plant biology, including plant
100 phenotypes under limiting phosphate conditions (Herrera Paredes et al., 2018), assembly of the
101 phylosphere microbiome (Bodenhausen et al., 2014; Carlström et al., 2019), or assembly cues
102 of the root microbiome (Bai et al., 2015; Finkel et al., 2020; Voges et al., 2019). SynComs
103 assembled from plant-associated bacteria have not yet been studied for their ability to assemble
104 stable communities *in vitro* in the absence of a host, although such a system would significantly
105 reduce the experimental complexity. Such *in vitro* systems have already been adopted in other
106 systems, for example for gut microbiota research (Li et al., 2019).
107 The assembly of a community from individual isolates is a complex process involving basic
108 metabolic (competitive or mutualistic) and chemical interactions between the different members
109 that form the community. In addition, environmental perturbations may destabilize a community,
110 shift its composition, or affect which individuals can establish themselves. The stability of
111 rhizospheric communities towards environmental perturbations is an important aspect of
112 rhizosphere biology. With the advent of precision agriculture and highly controlled growth
113 environments, engineering of the rhizosphere is an emerging topic that encompasses plant

biology, microbiology, microbial ecology, as well as genetic and biochemical biological disciplines (Dessaux et al., 2016; Ke et al., 2020).

Here, we investigated the impact of BX and their derivatives on bacterial members of the plant root and rhizosphere. We used the *AtRSphere* collection, derived from the root and rhizosphere of the model plant species *Arabidopsis thaliana* that includes around 180 culturable isolates distributed across four bacterial phyla (Bai et al., 2015) for dose-dependent *in vitro* responses to the BX APO and BOA, which can be found in soil surrounding BX-releasing plants.

A. thaliana is not a BX producer, therefore the ability of an isolate to colonize *A. thaliana* roots should be independent of its BX tolerance. In line with this assumption, our study revealed a wide range of growth responses, particularly to APO, among the *A. thaliana* derived *AtRSphere* collection. This occurred both within and across genera, ranging from complete insensitivity to strongly impacted growth. Information on the individual isolates' response guided our design of SynComs to investigate how BX and BX derivatives shape community assembly *in vitro.* We made use of the isolate-level diversity we observed in the collection with regards to BX exposure, to explore their potential to form communities differing in resilience to BX-mediated community perturbations. We found that the ability of an isolate to establish as a community member is often uncorrelated to growth in pure culture, and that sensitivity of an isolate to BX may change unpredictably when embedded in a community. Nevertheless, we also found that SynComs underwent compositional changes *in vitro* that reflected those previously observed in soil. Since the included isolates partially overlapped between generated SynComs, we conducted a comparative analysis to understand how chemical treatment and identity of member isolates shape the composition of *in vitro* communities.

136 # Results

137 ## BX derivatives selectively inhibit the growth of root associated
138 bacteria *in vitro*

139 To gain an overview of how benzoxazinoids and their derivatives affect individual plant-
140 associated bacteria, we screened the *AtRSphere* collection comprising 180 isolates of *A.*
141 *thaliana* rhizospheric bacteria (Bai et al., 2015) (Figure 1). We monitored the growth of each
142 isolate over 70 h in half-strength TSB medium after supplementation with either BOA (Figure
143 1A, inner heatmap) or APO (Figure 1A, outer heatmap), two plant-BX-derived compounds
144 commonly found in soil, and under control conditions (equivalent concentration of solvent only).
145 By determining cell density at regular intervals and comparing the area under the curve for the
146 control and BX treatments, we assessed each isolate's response to different compound
147 concentrations (Figure 1A).
148 The growth of most isolates was not inhibited by BOA, even at high concentrations of 100 µM.
149 Some isolates even seemed to benefit (darker color in Figure 1) from the presence of BOA
150 compared with control conditions; this was most consistent for isolates within the *Rhizobium* and
151 *Paenibacillus* genera (Figure 1B, C). However, such growth promotion was rare overall. This
152 might be attributable to the use of a nutrient-rich medium in this study, which would make BOA
153 superfluous as a potential energy source.
154 In stark contrast to the overall weak impact of BOA, exposure to APO severely inhibited growth
155 of 43% of the isolates (77/180 isolates grew to less than 50% of control levels in 50 µM APO)
156 (Figure 1A). Some isolates were insensitive to low APO concentrations but showed growth

157 inhibition at concentrations ≥10 μM, while others showed inhibition already at 5 μM APO (Figure
158 1). Generally, the impact of APO on growth was dose dependent. Overall, sensitivity to APO
159 appeared to be isolate-specific, as sensitivities varied as widely within as they did across
160 families and genera. APO-sensitive isolates (defined as showing <50% relative growth at 50 μM
161 APO) were present in all families covered by the *AtRSphere* collection (Figure 1A), with the
162 exception of the *Pseudomonadaceae* and *Alcaligenaceae* (Figure 1D, E). Within those clades
163 that contained APO-sensitive isolates, the response pattern did not follow an obvious
164 phylogenetic structure (16S rRNA-based phylogeny), indicating that sensitivity to APO is
165 species- or even isolate-specific within one genus.

166 Synthetic bacterial communities are structured by BX treatment

167 Since we were interested in the effect of BX on communities, we designed four different
168 SynComs based on the responses of the individual isolates: one that fully represented the
169 isolate collection at the genus level by randomly choosing one isolate per genus (referred to
170 hereafter as *random*) and three reduced-complexity SynComs (Supplemental Table 1). Of
171 these, the *tolerant* SynCom only contained isolates (max. one per genus) that had grown to at
172 least 50% of the control level in 50 μM APO. As can be seen in Figure 1A, several isolates that
173 were part of *tolerant* were also included in *random*. The *sensitive* SynCom consisted only of
174 isolates that had grown to less than 50% of control levels in 50 μM APO. Finally, the *mixed*
175 SynCom contained both APO-sensitive and APO-tolerant isolates (Figure 1A). To understand
176 the temporal and treatment-specific community dynamics, we grew each SynCom in three
177 different environments: control (supplemented with DMSO, the solvent used in the other two
178 treatments), 100 μM BOA, and 50 μM APO. We monitored SynCom composition in 24 h
179 intervals over 4 d via 16S rRNA sequencing (see methods).

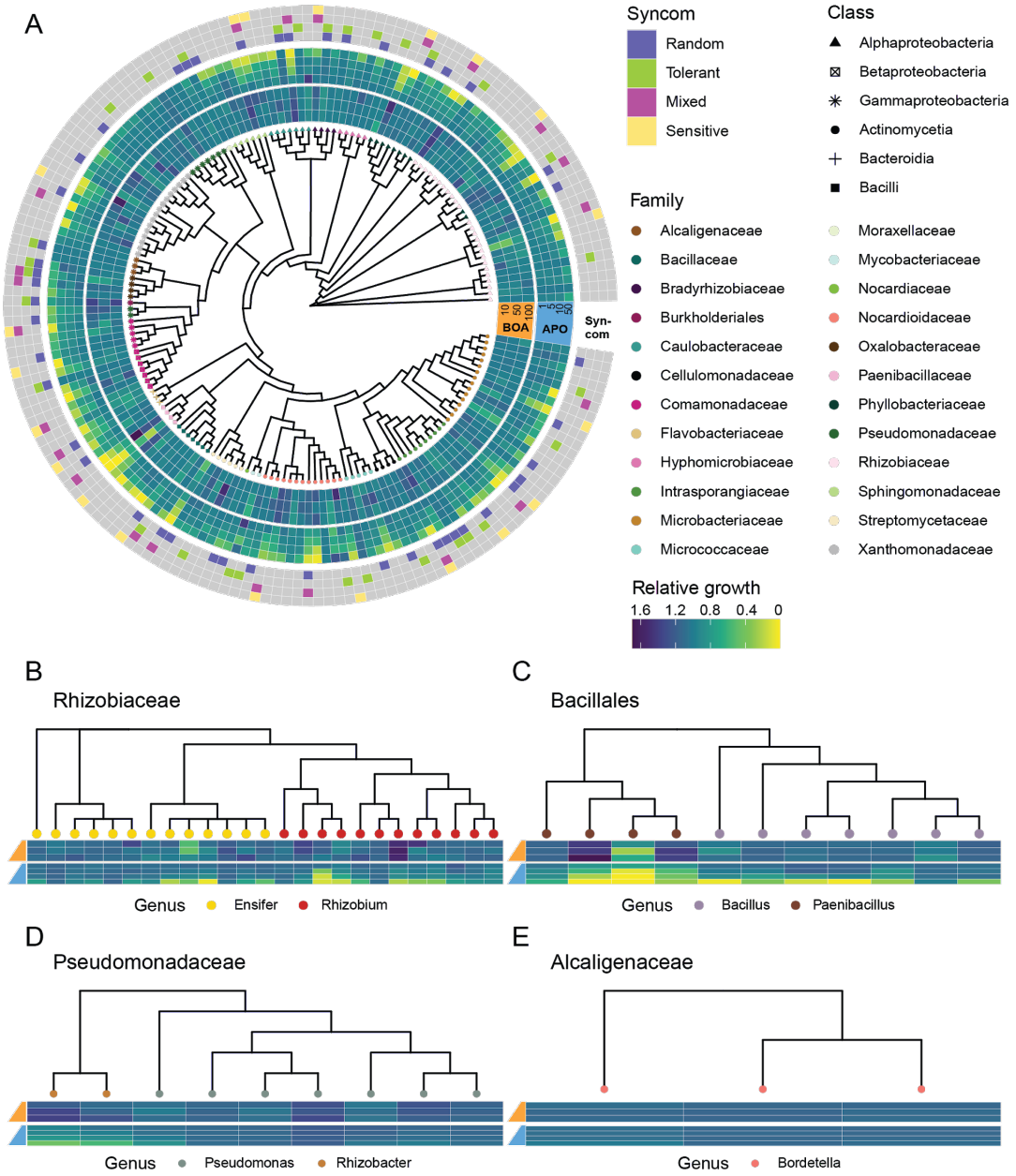

Figure 1. Isolate sensitivity to BX compounds and derivatives. A) Heatmap arranged around a circular phylogenetic tree computed from 16S rRNA sequences. Nodes represent isolates from the collection, node shape indicates taxonomic class, node color indicates taxonomic family. The inner heatmap displays average relative growth when treated with BOA (from inner to outer: 10 μM, 50 μM and 100 μM BOA, rings 1-3). The central heatmap displays relative growth upon APO treatment (inner to outer: 1 μM, 5 μM, 10 μM and 50 μM, rings 4-7). The outer heatmap indicates whether or not the isolate was selected as a member of one of the 4 synthetic communities (see main text for details). **B-E)** Sub-tree of isolates from the *Rhizobiaceae* family **(B)**, *Bacillales* order **(C)**, *Pseudomonadaceae* family **(D)**, and *Alcaligenaceae* family **(E)**; the heatmap displays relative growth in BOA (Orange, from top to bottom: 10 μM, 50 μM, 100 μM) and APO (Blue, from top to bottom: 1 μM, 5 μM, 10 μM and 50 μM). Node color represents taxonomic assignment at the genus level (legend below the heatmap).

192 As all bacteria analyzed here had originally been isolated from complex plant root microbiomes,
193 we first assessed to which degree they could reassemble into communities *in vitro* in the
194 absence of a host. Constrained correspondence analysis (CCA) of Jaccard distances calculated
195 from relative abundances revealed that SynComs assembled reproducibly (Figure 2A-D).
196 We next assessed if communities containing only APO-sensitive isolates would be more
197 strongly restructured by the addition of APO than one assembled only from APO-tolerant
198 isolates. Generally, we observed treatment-specific changes in all SynComs. Overall, BOA-
199 treated samples were similar to the control in all SynComs, with the exception of the *sensitive*
200 one. APO-treated samples clustered separately from both control and BOA (Figure 2 A-D). The
201 separation between APO and the remaining samples in the ordination was most obvious for the
202 *mixed* and *random* and less striking for the *tolerant* SynCom; it decreased over time in the
203 *sensitive* one (Figure 2 A-D).
204 We performed permutational multivariate analysis of variance (PERMANOVA) to see if we could
205 corroborate these observations. Treatment explained a significant proportion of variance in all
206 SynComs: 40% in *random*, 22% in *tolerant*, 75% in *mixed*, and 41% in *sensitive*. This means
207 that the proportion of between-sample variance explained by BX treatments was lowest in the
208 community assembled from APO-tolerant isolates. Time point explained a significant proportion
209 of variance in *random* and *tolerant* (31% and 33%, respectively) but not in *mixed* or *sensitive*
210 (Supplemental Table 2). We then performed another PERMANOVA analysis on each SynCom,
211 subsetted to a binary comparison between control and either APO or BOA treatment, to
212 estimate the amount of variance explained by the individual treatments (Supplemental Table 3).
213 This confirmed that most of the variance observed between treatments in each SynCom was
214 driven by APO (Figure 2A-D). The amount of variance explained by APO treatment was lowest
215 in the *tolerant* SynCom (22%), while APO treatment explained approx. 40% in *random* and
216 *sensitive* and 70% in *mixed* (Supplemental Table 3). In other words, the SynCom composed of
217 only the most APO-tolerant individual isolates showed the highest resilience to APO.

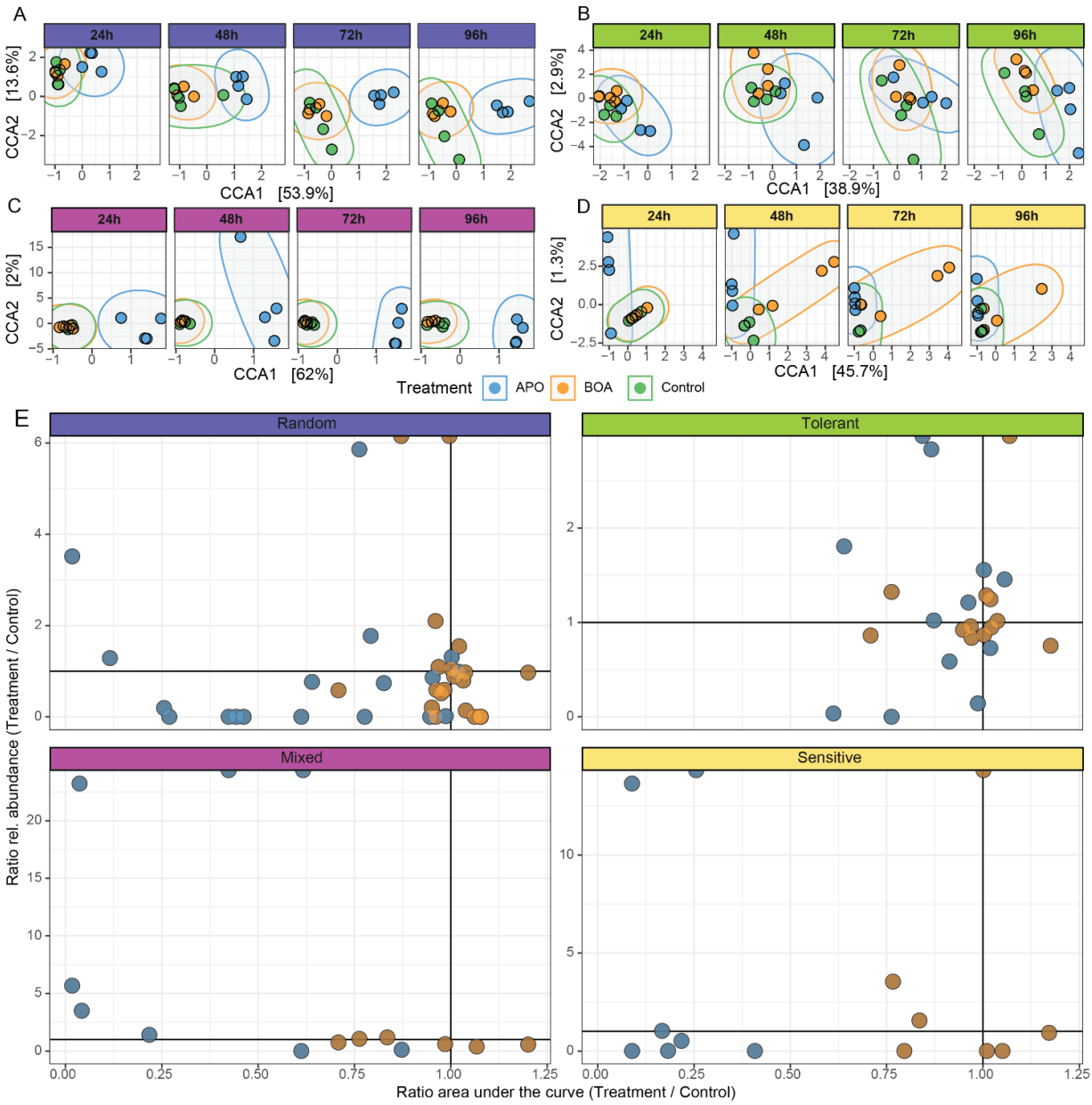

Figure 2. Community analysis. Constrained correspondence analysis (CCA, constrained by 'Treatment' and 'Time point') of the Jaccard distances computed on relative genus abundances for all samples. **A-D)** CCA per SynCom (**A**: random; **B**: tolerant; **C**: mixed; **D**: sensitive); faceted by time point (columns) and colored by treatment. **E)** Relationship between change in bacterial growth in the presence of BX compounds in pure culture (x-axis) plotted against the change in relative abundance when embedded in a community (y-axis) for APO (blue) and BOA (orange). Each dot shows the average change in relative abundance for one isolate across all time points.

Having confirmed that the different isolate mixtures reliably assembled into reproducible communities, we asked if within-sample species diversity (alpha-diversity) was affected by time or treatment by applying analysis of variance (ANOVA). In the *random*, *tolerant*, and *mixed*

230 SynComs, APO (but not BOA) treatment significantly reduced the total number of taxa at one or
231 more time points, while in the *sensitive* SynCom, the taxon number remained constant across
232 treatments and time points (Supplemental Figure 1, Supplemental Tables S4 and S5). However,
233 while the total number of taxa remained the same, different taxa were driven to extinction (ratio
234 of 0 on the relative abundance scale axis, Figure 2E) by the individual treatments, while the
235 presence of other taxa was specific for one of the compounds (appearing at the very top of each
236 panel in Figure 2E). Time alone, however, did not significantly influence the species number in
237 any of the SynComs. The Shannon measure of alpha diversity, which in addition to the number
238 of species also incorporates the evenness of species abundances, was significantly influenced
239 by both time and treatment (Supplemental Figure 2, Supplemental Table 5). While APO
240 treatment significantly increased Shannon diversity of the *mixed* and *tolerant* communities, it
241 decreased Shannon diversity of the *sensitive* one. In contrast, BOA significantly increased
242 Shannon diversity of the *sensitive* SynCom after 48 h (Supplemental Table 6).
243 Overall, there was no clear relationship between the growth of an isolate *in vitro* and the ability
244 of an isolate to establish itself as a SynCom member. In fact, some isolates that barely grew
245 when cultured individually reached relative abundances of >90% when grown in a community
246 (Figure 2E, *mixed* and *sensitive*, top left corner of the plot). The overall magnitude of magnitude
247 of change, excluding extinction in treatment or absence of control, in relative isolate abundance
248 was lowest in the *tolerant* SynCom (Figure 2E). The relative abundance ratios in the *tolerant*
249 community ranged from 0.03 to 2.8, while the lower bound of this range was lower (*random*:
250 0.0001; *mixed*: 0.005; *sensitive*: 0.008) and the upper bound was higher (*random*: 5.9; *mixed*:
251 23.2; *sensitive*: 13.6) in all other SynComs. This result indicates that isolates that were found in
252 all conditions in the *tolerant* SynCom were generally less affected in their relative abundance by
253 APO treatment, than isolates that were included in the other SynComs (Figure 2E).

Response of community-embedded isolates to BX treatment

Since previous studies reported a substantial impact of plant-derived BX on soil microbiota (Hu et al., 2018; Cotton et al., 2019; Kudjordjie et al., 2019; Cadot et al., 2020), we were interested in assessing if the reported effects could be recapitulated using reduced complexity communities *in vitro*. To understand which taxa drove the observed differences between treatments (Figure 2), and if similar changes occurred upon APO treatment in the different communities, we estimated the fold-change in taxon abundance per SynCom and time point between APO- and BOA-treated samples as well as between APO and control, and between BOA and control (Figure 3). In this first approach, we focused on those taxa that showed a significant fold-change between two treatments for at least one time point.

Overall, we observed APO-dependent shifts in relative abundance of different genera in all SynComs, the comparison of relative abundances between BOA and control conditions only yielded significant differences in the *sensitive* community.

Some genera were consistently reduced in APO-treated communities. These were *Bacillus* in *random* (Figure 3A)*, tolerant* (Figure 3B) and *sensitive* (Figure 3D), *Flavobacterium* in *random* (Figure 3A) and *mixed* (Figure 3C) and *Acidovorax* in every SynCom, irrespective of the particular isolate used (Fig 3A-D). Other genera thrived in APO-treated samples: *Lysobacter (*in *mixed* and *sensitive*) and *Hoeflea* (identical isolate Root268 in *random* and *sensitive*)*.* Only the genus *Microbacterium* displayed opposing behavior between SynComs: abundance was increased when treated with APO in *mixed* and *sensitive*, while abundance in the *tolerant* community was significant reduced in APO-treated samples at 48 h. While *Microbacterium* was significantly reduced in *tolerant* after 48 h (see confidence intervals in Fig 3B), it is possible that this is attributable to measurement error, considering that this isolate was only lowly abundant in this community.

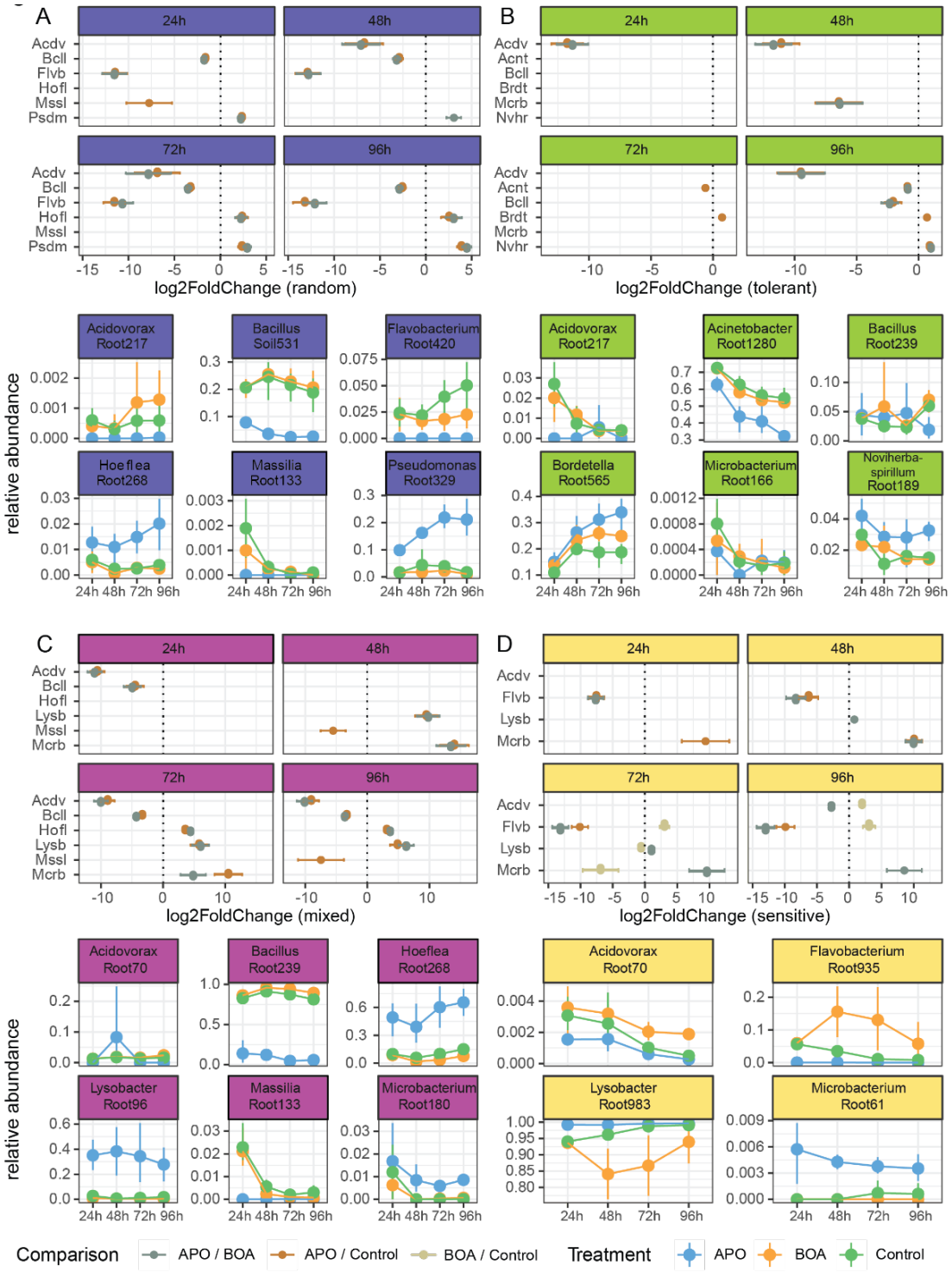

Figure 3: Treatment-specific and temporal isolate abundances in SynComs. Fold-changes between treatments and relative abundances of isolates that were significantly different for at least one time point, estimated by DESeq2. Plots are divided by SynCom: *random* **(A)**, *tolerant* **(B)**, *mixed* **(C)**, and *sensitive* **(D)**. In fold-change plots (top) only significant changes are shown for each time point. Line graphs (below) show relative abundance for all time points for isolates with significant fold-changes. Dots mark the mean across replicates, error bars indicate the 95% confidence interval.

Interactions between isolates are modulated by community members and chemical treatment

In the next approach, we wanted to move beyond comparing only treatment-specific effects and investigate whether interactions between community members were influenced by community context and chemical treatment. The assignment of isolates to the *random* community had been done blindly. However, several of the isolates included in the *random* community were also part of *tolerant* (Figure 1A). We therefore reasoned that differences in the relative abundance of these isolates between the two SynComs likely resulted from interactions with other, non-shared SynCom members. To test this hypothesis, we calculated Pearson's correlation between sequence counts assigned to isolates in each SynCom at 24 h and 96 h. We then constructed correlation networks per treatment and time point, including all correlations with an absolute $r > 0.5$. The networks for BOA and APO at the 24 h and 96 h time points are shown in Figure 4B, the remaining networks in Supplemental Figure 3.

The *random* and *tolerant* communities became more similar over time when treated with APO, overlapping in 5 genera (out of a total 8) included in the network, confirming the observation in Figure 2A. *Hoeflea* and *Rhodanobacter* were detectable only in the *random* SynCom, *Rhizobium* only in the *tolerant* SynCom. Some of the shared isolates were not detectable in APO but only in BOA and control conditions: *Massilia* Root133 was detected in the early time point, *Acidovorax* Root217 established itself at the late time point (Figure 4B).

When looking at the interactions between isolates, we observed that after treatment with APO, *Bordetella* Root565, *Noviherbaspirillum* Root189, and *Acinetobacter* Root1280 displayed strong, positive correlations after 96 h in both *tolerant* and *random* SynComs. This suggested that this group of isolates engaged in similar interactions, irrespective of the other isolates in the community. However, the relative abundance *Acinetobacter* Root1280 appeared to be more affected by APO treatment in the *tolerant* than in the *random* community (Figure 4A). Based on

the correlation networks, we propose that this differential behavior is related to the presence of different *Pseudomonas isolates* in those SynComs. *Pseudomonas* Root9 negatively correlated with *Acinetobacter* Root1280 in the APO- but not in the BOA-treated *tolerant* SynCom at 96 h. In fact, in the BOA-treated samples, this correlation was positive. In the APO-treated *random* SynCom, *Pseudomonas* Root329 was positively correlated with *Acinetobacter* Root1280 at 96h.

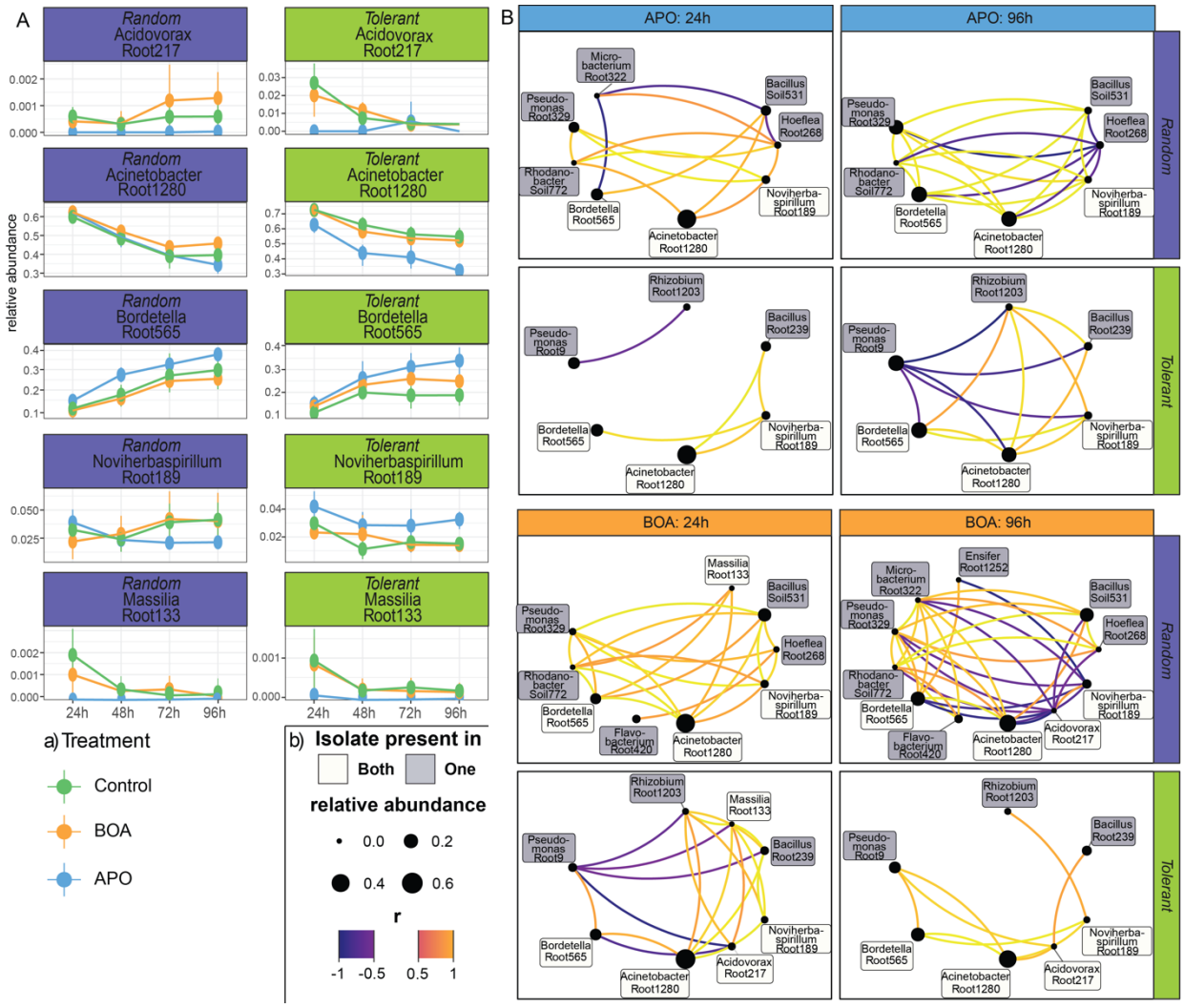

Figure 4: Differential isolate interactions in the *random* and *tolerant* SynComs are driven by isolate identity and chemical treatment. A) Relative abundance of isolates present in both SynComs, over time and by treatment. **B)** Pearson's correlations of isolate abundances in the *tolerant* and *random* SynComs. Each node represents one isolate; node size reflects relative abundance. Color of the node label indicates if an isolate was a member of both (white) or only one (grey) of the SynComs. Each edge indicates a correlation where |r| > 0.5 between two isolates; edge color indicates the correlation value, negative correlations have a blue hue, while positive correlations are orange to yellow.

Discussion

Diversity of BX sensitivity in culturable rhizosphere bacteria

In our screen of the *AtRSphere* collection for sensitivity to BX derivatives (Figure 1), we observed broad diversity of growth responses to BX exposure. While some clades were non-responsive to BOA and APO, we observed diverse responses in most clades. APO exerted a strong negative influence on the growth of some isolates. These findings are in line with previous results showing the antibiotic activity of APO on anaerobic microorganisms (Atwal et al., 1992). In our study, BOA influenced bacterial growth only marginally compared to APO, similar to what has been described for their effects on fungi and plants. In general, this corroborates the previously suggested relevance of APO, which is more stable than BOA in soil, in BX-mediated plant-environment interactions (Kumar et al., 1993; Schandry and Becker, 2020; Schulz et al., 2013; Schütz et al., 2019; Venturelli et al., 2015; Voloshchuk et al., 2020). However, our data showed that bacterial response to APO was largely isolate-specific and not dictated by phylogenetic relationship (Figure 1A). This indicates that even within genera, natural genetic diversity can result in substantial differences in BX sensitivity. Indeed, previous studies reported functional overlap related to responses to plant-derived compounds between isolates from different clades, while not all isolates of the same clade shared these functionalities (Bai et al., 2015; Harbort et al., 2020). The broad phylogenetic spectrum of the *AtRSphere* collection prevented the identification of genetic components underlying bacterial response to BOA and APO. However, the strongly differential responses we observed among closely related isolates warrant a more comprehensive analysis of the genetic basis of the BX response in the respective clades in future experiments.

345 One major advantage of the *AtRSphere* collection is that it was isolated from a non-BX-
346 producing host plant. The soil from which this collection was originally derived (Cologne soil)
347 was collected from an agricultural site, and in absence of a complete record of the field's history,
348 we cannot exclude that there might have been an input of BX in the past. Our findings on the
349 standing diversity of BX tolerance further imply that this diversity is maintained in plant-
350 associated bacteria, also in the absence of a BX-releasing host. Strain specific tolerance or
351 sensitivity to plant specialized metabolites may thus contribute to the colonization profiles
352 observed for different plant species, where the composition is similar at higher taxonomic ranks,
353 but some isolates show host preference (Bulgarelli et al., 2013; Schneijderberg et al., 2020)

354 Evaluation of bottom-up design strategy

355 Others have previously proposed that synthetic communities should be built with a focus on
356 functional features instead of on phylogenetic coverage (Lemanceau et al., 2017; Vorholt et al.,
357 2017). We employed a simple, function-guided strategy, compiling SynComs by binning
358 individual isolates based on a specific phenotype and contrasting these binned assemblies to a
359 randomly assembled SynCom. The decisive phenotype measured at the level of individual
360 isolates and used for binning them into SynComs was growth upon exposure to APO. The
361 phenotype measured at the community level, variance explained by treatment, was lowest
362 (22%) in the SynCom assembled solely from APO-tolerant isolates, indicating that resistance of
363 SynCom members leads to overall community resilience. While this approach worked well to
364 create an overall resilient community, the amount of variance explained by treatment was
365 similar in *random* and *sensitive* (~40%) and highest in the *mixed* SynCom (75%), indicating that
366 mixing tolerant and sensitive isolates does not necessarily result in a community with
367 intermediate resilience.

368 ## Stability of communities *in vitro*

369 Bacterial communities that assemble *in vitro* are less complex, with respect to the genera they
370 comprise, than those found on and around plant roots yet still contain a considerable number of
371 different isolates in coexistence. One might expect that in an *in vitro* system containing a
372 mixture of isolates, one isolate outgrows the others and reaches very high abundance. This
373 would mean that there are no interactions between the individual isolates and that growth rate is
374 a strong predictor of final abundance. We observed dominance of an isolate in the *sensitive*
375 community, where *Lysobacter* reached >90% relative abundance. However, upon the addition
376 of BOA we observed that *Flavobacterium* was able to establish itself at >10% relative
377 abundance (corresponding to an eight-fold increase over control). In the *mixed* community,
378 *Bacillus* reached >90% abundance in the BOA and control conditions; however, in the APO
379 treatment, *Bacillus* was strongly reduced in relative abundance, while *Hoeflea* and *Lysobacter*
380 proliferated. In all other SynComs, several isolates reproducibly formed a community, with
381 relative abundances staying within a narrow range across replicates but varying by orders of
382 magnitude between genera.
383 The growth of an isolate by itself was only poorly correlated with its ability to establish itself as a
384 SynCom member or with its relative abundance in a community (Figure 2E). In fact, several
385 isolates that grew poorly on their own reached high relative abundance when grown in
386 communities, possibly indicating facilitation by other members. However, it should be noted that
387 we confirmed a maximum of 15 isolates per SynCom by 16S rRNA sequencing.

BX dependent community alterations *in vitro* mimic those described in soil

Our work complements recent research efforts to understand the effect of benzoxazinoids on plant-associated microbiota in soil (Cadot et al., 2020; Cotton et al., 2019; Hu et al., 2018; Kudjordjie et al., 2019; Neal et al., 2012). Ultimately, for *in vitro* SynCom systems to be a useful model for plant microbiota research, they should behave similarly to microbiota in soil. BX constitute a prime system to assess this, as the influence of BX release on the root and rhizosphere microbiome has been investigated via mutant studies in different soils (Cadot et al., 2020; Cotton et al., 2019; Hu et al., 2018; Kudjordjie et al., 2019). Among the bacterial taxa that were found in different studies, *Flavobacteriales* were observed as depleted in multiple studies. Hu et al (Hu et al., 2018) found *Flavobacterium* depleted on the roots of BX-exuding plants and the surrounding soils when comparing wildtype and *bx1* mutant plants. Extending these observations, Cadot et al (Cadot et al., 2020) reported that *Flavobacteriaceae* were consistently depleted on roots of BX-producing plants, independent of soil type and location. Similarly, members of the *Flavobacteriales* family were more abundant on the roots of maize BX-synthesis mutants than on wildtype in another, independent study (Cotton et al., 2019). In all of the afore-mentioned studies, *Comamonadaceae* were also reported to be depleted on roots of BX-releasing plants when compared to BX-deficient mutants (Cadot et al., 2020; Cotton et al., 2019; Hu et al., 2018; Kudjordjie et al., 2019).

Our data show that the growth of *Flavobacterium* isolates was only slightly reduced across APO levels, with some isolates displaying mild sensitivity to BOA. However, *Flavobacterium* was significantly depleted from the *random* and *tolerant* SynComs once the community was exposed to APO. *Flavobacterium* was not found in the other two communities. Similarly, *Acidovorax* (*Comamonadaceae*) was found to be reduced in the APO treatment in all SynComs. Thus, even

412 though *in vitro* cultivation strongly differs from soils in physical and chemical parameters and in
413 overall complexity, our study suggests that plant-exudate-mediated effects on soil communities
414 can be recapitulated *in vitro*, highlighting the applicability of such reduced-complexity systems
415 for future studies. In addition, such simplified systems may aid in the identification of microbial
416 isolates that act as community keystones, or hubs, under specific chemical challenges in a short
417 experimental time frame (Carlström et al., 2019). These data can then be used as a basis for
418 the design of host-associated communities that are able to remain stable even in the presence
419 of toxic metabolites, which may increase plant productivity in mixed-cultivation settings.

420 Chemical stability of isolate interactions

421 Partial overlap in the communities that arose from the *random* and *tolerant* SynCom mixtures
422 allowed us to investigate to which degree the identity of community members influences the
423 interactions between isolates. The *random* and *tolerant* SynComs shared five isolates, three of
424 which were detectable in all treatments and time points. After 96 h, the *random* and *tolerant*
425 communities overlapped in 5 genera, including 3 identical isolates and differing representatives
426 of *Pseudomonas* and *Bacillus*. The identical isolates *Bordetella*, *Acinetobacter*, and
427 *Noviherbaspirillum* positively correlated in both SynComs, indicating that these isolates may
428 form a rather stable network *in vitro*. However, the influence of *Pseudomonas* on this network
429 was negative in the *tolerant* SynCom, while the *Pseudomonas* isolate in the *random* SynCom
430 was positively correlated with the network formed by *Acinetobacter*, *Bordetella*, and
431 *Noviherbasprillium*. This indicates that the exchange of a single isolate for a closely related
432 isolate from the same genus can have a broad influence on the overall community composition.
433 This supports the view that some community members can facilitate or compete with a larger
434 group of interacting members, i.e., acting as keystones (Banerjee et al., 2018), although this
435 ability seems to be variable within a clade. We speculate that understanding the connections

436 between environmental factors and the genetics underlying the ability of an isolate to function as
437 a key-stone would open up genetic engineering of community stability, for example by stacking
438 “key-stone genes” into one isolate. Such an isolate then could be used to stabilize communities
439 used as inoculants in agriculture.

440 Methods

441 Isolate profiling

442 Individual isolates were pre-cultured in ½ strength TSB medium in 96-Well 2 ml deep-well plates
443 (Semadeni) covered with a Breathe-Easy (Diversified Biotech) membrane until stationary phase
444 for 6 d at 28°C and 180 rpm. Cultures were then resuspended by pipetting up and down 10
445 times and inoculated into 96-well flat-bottom, transparent cell culture plates (Nunc), containing
446 either solvent control (DMSO), 1 µM APO, 5 µM APO, 10 µM APO, 50 µM APO, 10 µM BOA, 50
447 µM BOA or 100 µM BOA in ½-strength TSB. Different media were prepared by mixing a stock
448 containing the highest concentration of the respective chemical, with medium containing the
449 solvent at the same concentration (DMSO; 1:20.000). Pipetting was carried out using an Agilent
450 Bravo pipetting robot equipped with a 96-tip head. Plates were stacked without lids, with one
451 empty plate at the top and the bottom of the stack and placed into a BioTek plate stacker
452 connected to a BioTek Synergy2 plate reader. Plates were shaken for 120 s before reading, and
453 absorption (600 nm) was measured in each well. Plates were continuously shaken, measured,
454 and stacked over the course of at least 48 h per replicate. For each replicate, the relative growth
455 per isolate and condition was calculated by dividing the area under the growth curve (x = time in
456 minutes; y = increase in OD600) in the respective condition by the area under the growth curve
457 of the control condition. The experiment was carried out in eight replicates per condition.

458 # Synthetic bacterial communities

459 ## Design

460 To investigate to which degree the overall resilience of a bacterial community to chemical
461 changes is determined by the properties of its individual members, we followed two separate
462 design strategies. In the first strategy, we aimed at creating a diverse community spanning all
463 genera of the isolate collection. The *random* community was created by picking one random
464 isolate per genus.
465 In the second approach, we built communities based on the growth profiles of the individual
466 isolates. These communities span a limited number of genera, but the member growth profile is
467 more strictly defined than in the “full” community. One of the reduced representation
468 communities was created from isolates that grew to 75% to 100% of control conditions in 50µM
469 APO (*tolerant*). The other reduced community was assembled from isolates that grew to 0 to
470 25% of control in 50µM APO (*sensitive*). If there was more than one isolate per genus that
471 fulfilled the condition, we selected one at random. In addition, we compiled one limited
472 representation SynCom containing a mix of sensitive and tolerant isolates (*mixed*).

473 ## Cultivation and sequencing

474 Individual isolates were pre-cultured in ½-strength TSB medium in 96-Well 2ml deep-well plates
475 covered with a Breathe-Easy membrane (Diversified Biotech) with shaking at 28°C for 6 days
476 until stationary phase, as described previously (Bai et al., 2015). Individual cultures were
477 resuspended by pipetting up and down 10 times, and then 100 µL of each culture were mixed
478 with 10 mL ½-strength TSB medium containing solvent at the same concentration as the
479 treatment cultures (1:20.000 DMSO). 100 µL of the mixed culture were used to inoculate 20 mL
480 cultures containing either a solvent control (DMSO), 100 µM BOA, or 50 µM APO in 100 mL

481 Erlenmayer flasks. Flasks were cultured at 28°C, 180 rpm; 1 ml culture was sampled every 24
482 h. Sampled cultures were centrifuged at 12.000 rpm, the supernatant was discarded and the
483 pellet was stored at -70 °C until further use. DNA was extracted using the DNA PowerSoil kit
484 (Qiagen) following the standard protocol. 16S amplicons were generated according to the
485 Illumina 16S protocol, indexed using Nextera XT dual indexing (Illumina), and pooled per time
486 point for sequencing on a MiSeq (Paired end 300bp, Illumina).

487 Data analysis

488 RStudio with R version 4.0.2 was used for data analysis. Reads processed and ASVs were
489 inferred using the dada2 pipeline (Ben J. Callahan et al., 2016). Taxonomic assignment of ASVs
490 was done using SynCom specific 16SrRNA databases and agglomerated at the genus level.
491 ASVs that could not be assigned were discarded. Scripts used for data analysis are available at
492 https://github.com/nschan/BxSyncomMs. The following R packages were used with R version
493 4.0.2:
494 Tidyverse (Wickham et al., 2019), Broom (Robinson et al., 2019), dada2 (Benjamin J. Callahan
495 et al., 2016), DECIPHER (Wright, 2016), DESeq2 (Love et al., 2014), emmeans (Lenth et al.,
496 2019), ggforce (Pedersen, 2020a), ggthemes (Arnold, 2019), ggtree (Yu, 2020; Yu et al., 2018,
497 2017), gt (Iannone et al., 2019), igraph (Csardi and Nepusz, 2006), MESS (Ekstrøm, 2016),
498 multcomp (Hothorn et al., 2008), patchwork (Pedersen, 2020b), phangorn (Schliep et al., 2017;
499 Schliep, 2011), phyloseq (McMurdie and Holmes, 2013), vegan (Oksanen et al., 2019),
500 wesanderson (Ram and Wickham, 2018) in combination with some custom functions.

501 Data availability

502 Sequencing reads have been deposited to the European Nucleotide Archive (ENA;
503 www.ebi.ac.uk) under the accession no. PRJEB42439.

Acknowledgements

The authors gratefully acknowledge support from the Vienna BioCenter Core Facility (VBCF) Molecular Biology Services, especially Dr. Robert Heinen, the VBCF Media Kitchen, the VBCF Sequencing facility and the VBCF High Performance Computing facility. The authors also gratefully acknowledge the Leibniz Supercomputing Centre (LRZ) for funding this project by providing computing time on its Linux-Cluster and Rstudio Server.

The authors thank Eva Knoch and Patrick Hüther for constructive feedback on the manuscript, and Iacopo Gentile and Karina Weiser-Lobao for conducting preliminary experiments and for technical support. The authors also thank Stijn Staepen for help with the *AtRSphere* collection and Paul Schulze-Lefert for helpful discussion.

This work was funded by the Austrian Academy of Sciences (ÖAW) and the European Research Council (ERC) under the European Union's Horizon 2020 research and innovation programme (Grant agreement No. 716823, "FEAR-SAP").

Supplemental Material

Supplemental figures

Supplemental Figure 1. Observed alpha diversity

Supplemental Figure 2. Shannon diversity indices of the synthetic communities

Supplemental Figure 3. Correlation networks

Supplemental Tables

Supplemental Table 1. SynCom isolates

Supplemental Table 2. PERMANOVA

Supplemental Table 3. ANOVA: observed taxa

Supplemental Table 4. Observed diversity means and pairwise comparisons

Supplemental Table 5. ANOVA: Shannon Diversity

Supplemental Table 6. Shannon diversity means and pairwise comparisons

Literature

Anzai K, Isono K, Okuma K, Suzuki S. 1960. The new antibiotics, questiomycins A and B. *J Antibiot* **13**:125–132.

Arnold JB. 2019. ggthemes: Extra Themes, Scales and Geoms for “ggplot2.”

Atwal AS, Teather RM, Liss SN, Collins FW. 1992. Antimicrobial activity of 2-aminophenoxazin-3-one under anaerobic conditions. *Can J Microbiol* **38**:1084–1088.

Bai Y, Müller DB, Srinivas G, Garrido-Oter R, Potthoff E, Rott M, Dombrowski N, Münch PC, Spaepen S, Remus-Emsermann M, Hüttel B, McHardy AC, Vorholt JA, Schulze-Lefert P. 2015. Functional overlap of the Arabidopsis leaf and root microbiota. *Nature* 1–19.

Banerjee S, Schlaeppi K, van der Heijden MGA. 2018. Keystone taxa as drivers of microbiome structure and functioning. *Nat Rev Microbiol* **16**:567–576.

Belz RG, Hurle K. 2005. Differential exudation of two benzoxazinoids--one of the determining factors for seedling allelopathy of Triticeae species. *J Agric Food Chem* **53**:250–261.

Bodenhausen N, Bortfeld-Miller M, Ackermann M, Vorholt JA. 2014. A synthetic community approach reveals plant genotypes affecting the phyllosphere microbiota. *PLoS Genet* **10**:e1004283.

Bulgarelli D, Rott M, Schlaeppi K, Ver Loren van Themaat E, Ahmadinejad N, Assenza F, Rauf P, Huettel B, Reinhardt R, Schmelzer E, Peplies J, Gloeckner FO, Amann R, Eickhorst T, Schulze-Lefert P. 2012. Revealing structure and assembly cues for Arabidopsis root-inhabiting bacterial microbiota. *Nature* **488**:91–95.

Bulgarelli D, Schlaeppi K, Spaepen S, van Themaat EVL, Schulze-Lefert P. 2013. Structure and Functions of the Bacterial Microbiota of Plants. *Annu Rev Plant Biol* **64**:807–838.

Cadot S, Guan H, Bigalke M, Walser J-C, Jander G, Erb M, van der Heijden M, Schlaeppi K. 2020. Specific and conserved patterns of microbiota-structuring by maize benzoxazinoids in the field. *bioRxiv*. doi:10.1101/2020.05.03.075135

Callahan BJ, McMurdie PJ, Rosen MJ, Han AW, Johnson AJA, Holmes SP. 2016. DADA2: High-resolution sample inference from Illumina amplicon data. *Nat Methods* **13**:581–583.

Callahan BJ, Sankaran K, Fukuyama JA, McMurdie PJ, Holmes SP. 2016. Bioconductor Workflow for Microbiome Data Analysis: from raw reads to community analyses. *F1000Res* **5**:1492.

Carlström CI, Field CM, Bortfeld-Miller M, Müller B, Sunagawa S, Vorholt JA. 2019. Synthetic microbiota reveal priority effects and keystone strains in the Arabidopsis phyllosphere. *Nat Ecol Evol* **3**:1445–1454.

Cheng C, Othman EM, Fekete A, Krischke M, Stopper H, Edrada-Ebel R, Mueller MJ, Hentschel U, Abdelmohsen UR. 2016. Strepoxazine A, a new cytotoxic phenoxazin from the marine sponge-derived bacterium Streptomyces sp. SBT345. *Tetrahedron Lett* **57**:4196–4199.

Cotton TEA, Pétriacq P, Cameron DD, Meselmani MA, Schwarzenbacher R, Rolfe SA, Ton J. 2019. Metabolic regulation of the maize rhizobiome by benzoxazinoids. *ISME J*. doi:10.1038/s41396-019-0375-2

Csardi G, Nepusz T. 2006. The igraph software package for complex network research. *InterJournal*.

De Roy K, Marzorati M, Van den Abbeele P, Van de Wiele T, Boon N. 2014. Synthetic microbial ecosystems: an exciting tool to understand and apply microbial communities. *Environ Microbiol* **16**:1472–1481.

Dessaux Y, Grandclément C, Faure D. 2016. Engineering the Rhizosphere. *Trends Plant Sci* **21**:266–278.

Ekstrøm C. 2016. MESS: Miscellaneous Esoteric Statistical Scripts.

Finkel OM, Salas-González I, Castrillo G, Conway JM, Law TF, Teixeira PJPL, Wilson ED, Fitzpatrick CR, Jones CD, Dangl JL. 2020. A single bacterial genus maintains root growth in a complex microbiome. *Nature*. doi:10.1038/s41586-020-2778-7

Fitzpatrick CR, Salas-González I, Conway JM, Finkel OM, Gilbert S, Russ D, Teixeira PJPL, Dangl JL. 2020. The Plant Microbiome: From Ecology to Reductionism and Beyond. *Annu Rev Microbiol*. doi:10.1146/annurev-micro-022620-014327

Frey M, Chomet P, Glawischnig E, Stettner C, Grün S, Winklmair A, Eisenreich W, Bacher A, Meeley RB, Briggs SP, Simcox K, Gierl A. 1997. Analysis of a chemical plant defense mechanism in grasses. *Science* **277**:696–699.

Handrick V, Robert CAM, Ahern KR, Zhou S, Machado RAR, Maag D, Glauser G, Fernandez-Penny FE, Chandran JN, Rodgers-Melnik E, Schneider B, Buckler ES, Boland W, Gershenzon J, Jander G, Erb M, Köllner TG. 2016. Biosynthesis of 8-O-Methylated Benzoxazinoid Defense Compounds in Maize. *Plant Cell* **28**:1682–1700.

Harbort CJ, Hashimoto M, Inoue H, Niu Y, Guan R, Rombolà AD, Kopriva S, Mathias J E E, Sattely ES, Garrido-Oter R, Schulze-Lefert P. 2020. Root-Secreted Coumarins and the Microbiota Interact to Improve Iron Nutrition in Arabidopsis. *Cell Host Microbe* **0**. doi:10.1016/j.chom.2020.09.006

Herrera Paredes S, Gao T, Law TF, Finkel OM, Mucyn T, Teixeira PJPL, Salas González I, Feltcher ME, Powers MJ, Shank EA, Jones CD, Jojic V, Dangl JL, Castrillo G. 2018. Design of synthetic bacterial communities for predictable plant phenotypes. *PLoS Biol* **16**:e2003962.

Hothorn T, Bretz F, Westfall P. 2008. Simultaneous inference in general parametric models. *Biom J* **50**:346–363.

Hu L, Mateo P, Ye M, Zhang X, Berset JD, Handrick V, Radisch D, Grabe V, Köllner TG, Gershenzon J, Robert CAM, Erb M. 2018. Plant iron acquisition strategy exploited by an insect herbivore. *Science* **361**:694–697.

Hu L, Robert CAM, Cadot S, Zhang X, Ye M, Li B, Manzo D, Chervet N, Steinger T, van der Heijden MGA, Schlaeppi K, Erb M. 2018. Root exudate metabolites drive plant-soil feedbacks on growth and defense by shaping the rhizosphere microbiota. *Nat Commun* **9**:2738.

Iannone R, Cheng J, Schloerke B. 2019. gt: Easily Create Presentation-Ready Display Tables. R package version 0.1. 0.

Imai S, Shimazu A, Furihata K, Furihata K, Hayakawa Y, Seto H. 1990. Isolation and structure of a new phenoxazine antibiotic, exfoliazone, produced by Streptomyces exfoliatus. *J Antibiot* **43**:1606–1607.

Jacoby RP, Koprivova A, Kopriva S. 2020. Pinpointing secondary metabolites that shape the composition and function of the plant microbiome. *J Exp Bot*. doi:10.1093/jxb/eraa424

Ke J, Wang B, Yoshikuni Y. 2020. Microbiome Engineering: Synthetic Biology of Plant-Associated Microbiomes in Sustainable Agriculture. *Trends Biotechnol*. doi:10.1016/j.tibtech.2020.07.008

Koprivova A, Schuck S, Jacoby RP, Klinkhammer I, Welter B, Leson L, Martyn A, Nauen J, Grabenhorst N, Mandelkow JF, Zuccaro A, Zeier J, Kopriva S. 2019. Root-specific camalexin biosynthesis controls the plant growth-promoting effects of multiple bacterial strains. *Proc Natl Acad Sci U S A*. doi:10.1073/pnas.1818604116

Kudjordjie EN, Sapkota R, Steffensen SK, Fomsgaard IS, Nicolaisen M. 2019. Maize synthesized benzoxazinoids affect the host associated microbiome. *Microbiome* **7**:59.

Kumar P, Gagliardo RW, Chilton WS. 1993. Soil transformation of wheat and corn metabolites mboa and DIM2BOA into aminophenoxazinones. *J Chem Ecol* **19**:2453–2461.

Lebeis SL, Paredes SH, Lundberg DS, Breakfield N, Gehring J, McDonald M, Malfatti S, Glavina del Rio T, Jones CD, Tringe SG, Dangl JL. 2015. Salicylic acid modulates colonization of the root microbiome by specific bacterial taxa. *Science* **349**:860–864.

Lemanceau P, Blouin M, Muller D, Moënne-Loccoz Y. 2017. Let the Core Microbiota Be Functional. *Trends Plant Sci* **22**:583–595.
Lenth R, Singmann H, Love J, Buerkner P, Herve M. 2019. emmeans: Estimated Marginal Means, aka Least-Squares Means (Version 1.3. 4).
Li L, Abou-Samra E, Ning Z, Zhang X, Mayne J, Wang J, Cheng K, Walker K, Stintzi A, Figeys D. 2019. An in vitro model maintaining taxon-specific functional activities of the gut microbiome. *Nat Commun* **10**:4146.
Liu Y-X, Qin Y, Bai Y. 2019. Reductionist synthetic community approaches in root microbiome research. *Curr Opin Microbiol* **49**:97–102.
Love MI, Huber W, Anders S. 2014. Moderated estimation of fold change and dispersion for RNA-seq data with DESeq2. *Genome Biol* **15**:550.
Macías FA, Oliveros-Bastidas A, Marín D, Castellano D, Simonet AM, Molinillo JMG. 2005. Degradation studies on benzoxazinoids. Soil degradation dynamics of (2R)-2-O-beta-D-glucopyranosyl-4-hydroxy-(2H)- 1,4-benzoxazin-3(4H)-one (DIBOA-Glc) and its degradation products, phytotoxic allelochemicals from Gramineae. *J Agric Food Chem* **53**:554–561.
Macías FA, Oliveros-Bastidas A, Marín D, Castellano D, Simonet AM, Molinillo JMG. 2004. Degradation Studies on Benzoxazinoids. Soil Degradation Dynamics of 2,4-Dihydroxy-7-methoxy-(2 H)-1,4-benzoxazin-3(4 H)-one (DIMBOA) and Its Degradation Products, Phytotoxic Allelochemicals from Gramineae. *J Agric Food Chem* **52**:6402–6413.
Maier L, Pruteanu M, Kuhn M, Zeller G, Telzerow A, Anderson EE, Brochado AR, Fernandez KC, Dose H, Mori H, Patil KR, Bork P, Typas A. 2018. Extensive impact of non-antibiotic drugs on human gut bacteria. *Nature* **555**:623–628.
McMurdie PJ, Holmes S. 2013. phyloseq: an R package for reproducible interactive analysis and graphics of microbiome census data. *PLoS One* **8**:e61217.
Neal AL, Ahmad S, Gordon-Weeks R, Ton J. 2012. Benzoxazinoids in root exudates of maize attract Pseudomonas putida to the rhizosphere. *PLoS One* **7**:e35498.
Oksanen J, Blanchet FG, Friendly M, Kindt R, Legendre P, McGlinn D, Minchin PR, O'Hara RB, Simpson GL, Solymos P, Stevens MHH, Szoecs E, Wagner H. 2019. vegan: Community Ecology Package.
Pedersen TL. 2020a. ggforce: Accelerating "ggplot2."
Pedersen TL. 2020b. patchwork: The Composer of Plots.
Ram K, Wickham H. 2018. wesanderson: A Wes Anderson Palette Generator.
Robert CAM, Veyrat N, Glauser G, Marti G, Doyen GR, Villard N, Gaillard MDP, Köllner TG, Giron D, Body M, Babst BA, Ferrieri RA, Turlings TCJ, Erb M. 2011. A specialist root herbivore exploits defensive metabolites to locate nutritious tissues. *Ecol Lett* **14**:55–64.
Robinson D, Hayes A, Couch S. 2019. Broom: Convert statistical objects into tidy tibbles.
Schandry N, Becker C. 2020. Allelopathic Plants: Models for Studying Plant–Interkingdom Interactions. *Trends Plant Sci* **25**:176–185.
Schliep, Klaus, Potts, J. A, Morrison, A. D, Grimm, W. G. 2017. Intertwining phylogenetic trees and networks. *Methods in Ecology and Evolution*. doi:10.1111/2041-210X.12760
Schliep KP. 2011. phangorn: phylogenetic analysis in R. *Bioinformatics*. doi:10.1093/bioinformatics/btq706
Schneijderberg M, Cheng X, Franken C, de Hollander M, van Velzen R, Schmitz L, Heinen R, Geurts R, van der Putten WH, Bezemer TM, Bisseling T. 2020. Quantitative comparison between the rhizosphere effect of Arabidopsis thaliana and co-occurring plant species with a longer life history. *ISME J*. doi:10.1038/s41396-020-0695-2
Schulz M, Marocco A, Tabaglio V, Macias FA, Molinillo JMG. 2013. Benzoxazinoids in rye allelopathy - from discovery to application in sustainable weed control and organic farming. *J Chem Ecol* **39**:154–174.
Schütz V, Bigler L, Girel S, Laschke L, Sicker D, Schulz M. 2019. Conversions of

Benzoxazinoids and Downstream Metabolites by Soil Microorganisms. *Frontiers in Ecology and Evolution* **7**:238.

Stringlis IA, Yu K, Feussner K, de Jonge R, Van Bentum S, Van Verk MC, Berendsen RL, Bakker PAHM, Feussner I, Pieterse CMJ. 2018. MYB72-dependent coumarin exudation shapes root microbiome assembly to promote plant health. *Proc Natl Acad Sci U S A*. doi:10.1073/pnas.1722335115

Trivedi P, Leach JE, Tringe SG, Sa T, Singh BK. 2020. Plant-microbiome interactions: from community assembly to plant health. *Nat Rev Microbiol*. doi:10.1038/s41579-020-0412-1

Venturelli S, Belz RG, Kamper A, Berger A, von Horn K, Wegner A, Bocker A, Zabulon G, Langenecker T, Kohlbacher O, Barneche F, Weigel D, Lauer UM, Bitzer M, Becker C. 2015. Plants Release Precursors of Histone Deacetylase Inhibitors to Suppress Growth of Competitors. *Plant Cell* **27**:3175–3189.

Venturelli S, Petersen S, Langenecker T, Weigel D, Lauer UM, Becker C. 2016. Allelochemicals of the phenoxazinone class act at physiologically relevant concentrations. *Plant Signal Behav* **11**:e1176818.

Voges MJEEE, Bai Y, Schulze-Lefert P, Sattely ES. 2019. Plant-derived coumarins shape the composition of an Arabidopsis synthetic root microbiome. *Proc Natl Acad Sci U S A* **116**:12558–12565.

Voloshchuk N, Schütz V, Laschke L, Gryganskyi AP, Schulz M. 2020. The Trichoderma viride F-00612 consortium tolerates 2-amino-3H-phenoxazin-3-one and degrades nitrated benzo[d]oxazol-2(3H)-one. *Chemoecology*. doi:10.1007/s00049-020-00300-w

Vorholt JA, Vogel C, Carlström CI, Müller DB. 2017. Establishing Causality: Opportunities of Synthetic Communities for Plant Microbiome Research. *Cell Host Microbe* **22**:142–155.

Vrancken G, Gregory AC, Huys GRB, Faust K, Raes J. 2019. Synthetic ecology of the human gut microbiota. *Nat Rev Microbiol* **17**:754–763.

Wickham H, Averick M, Bryan J, Chang W, McGowan L, François R, Grolemund G, Hayes A, Henry L, Hester J, Kuhn M, Pedersen T, Miller E, Bache S, Müller K, Ooms J, Robinson D, Seidel D, Spinu V, Takahashi K, Vaughan D, Wilke C, Woo K, Yutani H. 2019. Welcome to the Tidyverse. *JOSS* **4**:1686.

Wright ES. 2016. Using DECIPHER v2. 0 to analyze big biological sequence data in R. *R J* **8**.

Yu G. 2020. Using ggtree to Visualize Data on Tree-Like Structures. *Current Protocols in Bioinformatics*. doi:10.1002/cpbi.96

Yu G, Lam TT-Y, Zhu H, Guan Y. 2018. Two methods for mapping and visualizing associated data on phylogeny using ggtree. *Molecular Biology and Evolution*. doi:10.1093/molbev/msy194

Yu G, Smith D, Zhu H, Guan Y, Lam TT-Y. 2017. ggtree: an R package for visualization and annotation of phylogenetic trees with their covariates and other associated data. *Methods in Ecology and Evolution*. doi:10.1111/2041-210X.12628